Molecular Therapy
Nucleic Acids
Original Article

Adeno-Associated Viral Vector-Mediated mTOR Inhibition by Short Hairpin RNA Suppresses Laser-Induced Choroidal Neovascularization

Tae Kwann Park,[1,2,6] Si Hyung Lee,[1,2,6] Jun Sub Choi,[3] Seung Kwan Nah,[1,2] Hee Jong Kim,[3] Ha Yan Park,[2] Heuiran Lee,[4] Steven Hyun Seung Lee,[4] and Keerang Park[5]

[1]Department of Ophthalmology, Soonchunhyang University, College of Medicine, Cheonan 31151, Republic of Korea; [2]Department of Ophthalmology, Soonchunhyang University Hospital Bucheon, Bucheon 14584, Republic of Korea; [3]Cdmogen Co., Ltd., Cheongju 28751, Republic of Korea; [4]Department of Microbiology, Cellular Dysfunction Research Center, Asan Medical Center, University of Ulsan, College of Medicine, Seoul 05505, Republic of Korea; [5]Department of Biopharmacy, Chungbuk Health & Science University, Cheongju, Chungbuk 28150, Republic of Korea

Choroidal neovascularization (CNV) is the defining characteristic feature of the wet subtype of age-related macular degeneration (AMD) and may result in irreversible blindness. Based on anti-vascular endothelial growth factor (anti-VEGF), the current therapeutic approaches to CNV are fraught with difficulties, and mammalian target of rapamycin (mTOR) has recently been proposed as a possible therapeutic target, although few studies have been conducted. Here, we show that a recombinant adeno-associated virus-delivered mTOR-inhibiting short hairpin RNA (rAAV-mTOR shRNA), which blocks the activity of both mTOR complex 1 and 2, represents a promising therapeutic approach for the treatment of CNV. Eight-week-old male C57/B6 mice were treated with the short hairpin RNA (shRNA) after generating CNV lesions in the eyes via laser photocoagulation. The recombinant adeno-associated virus (rAAV) delivery vehicle was able to effectively transduce cells in the inner retina, and significantly fewer inflammatory cells and less extensive CNV were observed in the animals treated with rAAV-mTOR shRNA when compared with control- and rAAV-scrambled shRNA-treated groups. Presumably related to the reduction of CNV, increased autophagy was detected in CNV lesions treated with rAAV-mTOR shRNA, whereas significantly fewer apoptotic cells detected in the outer nuclear layer around the CNV indicate that mTOR inhibition may also have neuroprotective effects. Taken together, these results demonstrate the therapeutic potential of mTOR inhibition, resulting from rAAV-mTOR shRNA activity, in the treatment of AMD-related CNV.

INTRODUCTION

Age-related macular degeneration (AMD) is a leading cause of irreversible blindness among the elderly of industrialized countries, affecting approximately 50 million people worldwide.[1,2] AMD presents itself as two distinct subtypes, dry and wet AMD. Dry AMD is characterized by geographic atrophy of the central retina, whereas wet AMD is identified by the formation of choroidal neovascularization (CNV).[3] In wet AMD patients, development of CNV can lead to macular edema, which results in the destruction of retinal structures and irreversible loss of vision. Currently, the main strategy for the treatment of wet AMD is based on neutralizing vascular endothelial growth factor (VEGF), either as a monotherapy or in conjunction with photodynamic therapy.[4,5] However, in addition to the economic burden of these repeated monthly treatments posing an obstacle to patient compliance,[6] the more challenging issue of therapy resistance means a need exists for the development of a new, long-lasting, disease-modifying therapy.

Mammalian target of rapamycin (mTOR) has been suggested as a therapeutic target for various human diseases, including cancer, type 2 diabetes, obesity, and neurologic disorders.[7–9] mTOR is a serine-threonine protein kinase that exists in nearly every eukaryotic cell and is a master regulator of cellular metabolism and cell growth. The mTOR pathway signals through two distinct complexes, mTOR complex 1 (mTORC1) and mTORC2. mTORC1, which consists of RAPTOR, PRAS40, and mLST8 proteins, is sensitive to rapamycin and is responsible for cell growth and proliferation, angiogenesis, synthesis of protein and lipid, and autophagy regulation.[10,11] mTORC2 contains RICTOR, PROCTOR1/2, and mLST8 as companion proteins and is closely related to the AKT pathway, because it phosphorylates AKT.[11] While mTORC1 signaling is relatively well understood, the functions of mTORC2 have not been widely investigated, and only recently has its critical roles in cytoskeletal organization, regulation of cell survival, and promotion of neovascularization been

Received 8 February 2017; accepted 29 May 2017;
http://dx.doi.org/10.1016/j.omtn.2017.05.012.

[6]These authors contributed equally to this work.

Correspondence: Tae Kwann Park, Department of Ophthalmology, Soonchunhyang University Hospital Bucheon, 170 Jomaru-ro, Wonmi-gu, Bucheon 14584, Republic of Korea.
E-mail: tkpark@schmc.ac.kr
Correspondence: Keerang Park, Department of Biopharmacy, Chungbuk Health & Science University, 10 Deokam-gil, Naesu-eup, Cheongwon-gu, Cheongju-si, Chungbuk 28150, Republic of Korea.
E-mail: krpark@chsu.ac.kr

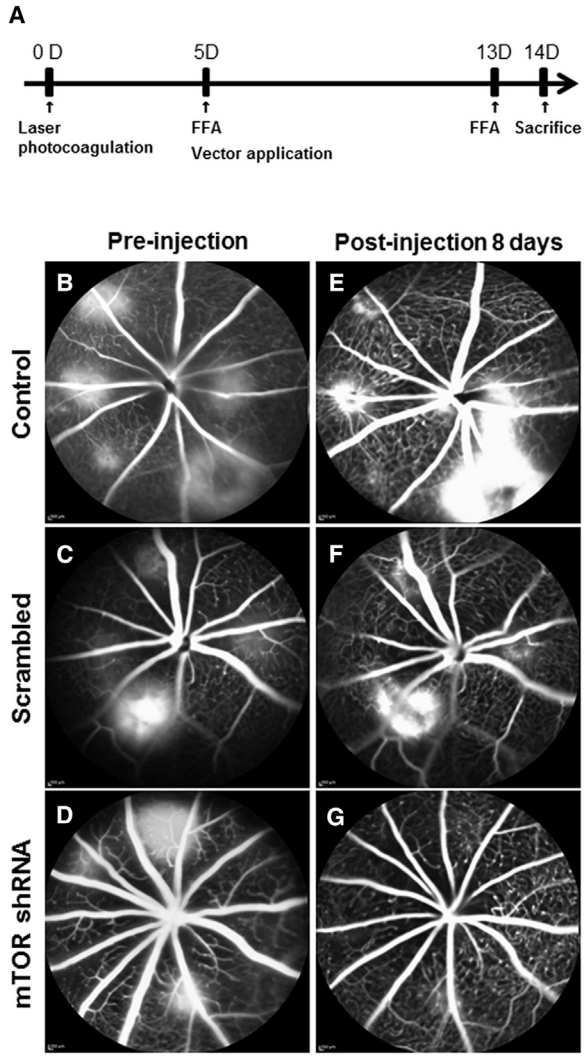

Figure 1. Experiment Protocol Schematic and Fundus Fluorescent Angiography Images Captured Pre- and Post-injection

All mice underwent laser photocoagulation (LP) at day 0. FFA images were captured 5 days post-LP immediately before intravitreal viral vector administration. (A) 13 days post-LP, FFA was performed again and the animals were sacrificed 1 day later. (B–D) Pre-injection FFA exhibited dye leakage at laser spots for all three groups (B, control; C, scrambled; D, mTOR shRNA), indicating CNV progression. (E–G) Eight days after vector administration, images from the control (E) and rAAV-scramble shRNA-injected mice (F) retained fluorescence leakage around CNV lesions, whereas the rAAV-mTOR shRNA-treated group exhibited CNV regression (G).

revealed.[12–14] Furthermore, deregulation of the mTOR signaling pathway leads to the development of several human diseases, because it is directly related to abnormalities in cell proliferation and survival processes.[7]

A number of studies have attempted to elucidate the role of the mTOR pathway in retinal cells. mTOR was shown to be a critical factor in the angiogenesis processes of various retinal pathologic conditions, including AMD, retinopathy of prematurity, and diabetic retinopathy.[15–17] Other recent studies demonstrated that autophagy induced by mTOR inhibition promoted the survival of retinal pigment epithelial (RPE) cells under toxic conditions,[18–20] indicating that the development of new therapeutic modalities for managing AMD may crucially include mTOR signaling pathway regulation.

Recombinant adeno-associated viruses (rAAVs) have shown promise as a vector for the in vivo delivery of gene-based drugs, and recent clinical successes with AAV vectors in treating Leber congenital amaurosis suggest that they may serve as a suitable platform for treating various ocular diseases.[21–24] Using mouse models, we previously demonstrated the enhanced transduction of intravitreally administered AAVs to various retinal cells, including RPE cells, upon retinal laser photocoagulation,[25,26] showing that the transduction of AAV vectors may be enhanced by the inflammatory or pathological state of the retina. As such, the efficient transduction of AAV vectors may be possible in diseased retinas, even for deep-lying RPE cells.

Recently, we designed a multispecies-compatible mTOR small interfering RNA (siRNA) sequence using a self-developed program, CAPSID (Convenient Application Program for siRNA Design),[27] that directly interferes with the mTOR signaling pathway by blocking both mTORC1 and mTORC2, and demonstrated in vivo that antitumor effects can be achieved by this rAAV-delivered mTOR-inhibiting short hairpin RNA (shRNA) (rAAV-mTOR shRNA).[28] Here, rAAV-mTOR shRNA was used to investigate whether mTOR inhibition suppresses laser-induced CNV in mouse chorioretinal tissue, and in addition to a substantial suppression of CNV, rAAV-mTOR shRNA-treated retinas exhibited decreased local inflammation and enhanced autophagic activity in CNV lesions.

RESULTS

Regression of CNV Leakage

Fundus fluorescein angiography (FFA) was performed 5 days after laser photocoagulation to observe vascular leakage and the establishment of new vessels. This was repeated at 13 days after laser photocoagulation to observe the therapeutic effects of rAAV-mTOR shRNA, which was injected intravitreally 5 days after laser photocoagulation (Figure 1A). FFA 5 days post-laser photocoagulation confirmed the establishment of CNV lesions, seen as well-defined hyperfluorescent leaking spots (Figures 1B–1D). These persisted in animals injected with either 0.1% PBS or rAAV-scrambled shRNA (Figures 1E and 1F), whereas FFA images taken from those animals treated with rAAV-mTOR shRNA showed a marked regression of leakage from the CNV lesions (Figure 1G).

Transduction of Vector to Endothelial Cells in CNV

Intravitreally administered self-complementary adeno-associated virus serotype 2 (scAAV2) vectors are known to transduce inner retinal cells in wild-type mice, including retinal ganglion cells and cells in the inner nuclear layer.[25] This is confirmed here, and in addition to the inner retinal cells, CD31-positive endothelial cells in the laser-induced CNV lesions also exhibited the transduction of rAAV-mTOR shRNA expressing GFP (Figure 2).

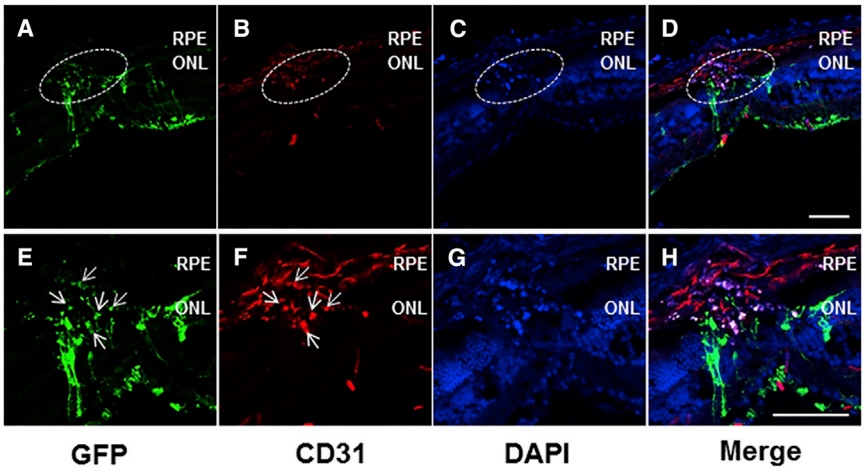

Figure 2. Efficient Vector Transduction Exhibited in Transverse Retinal Sections

(A–H) GFP expression was detectable throughout the retinal layers (A–D) (original magnification ×2 in E–H) from retinal ganglion cells to CD31-positive endothelial cells present in areas where choroidal neovascularization (CNV) was induced via laser photocoagulation (arrows in E and F), demonstrating the efficient transduction of rAAV-mTOR shRNA into cells of the outermost retinal layer. Scale bars, 100 μm. ONL, outer nuclear layer; RPE, retinal pigment epithelium.

mTOR Expression in Laser-Induced CNV

To determine the effect of the mTOR shRNA on mTOR activity, we first evaluated mTOR expression in all four groups of mice, including the negative control. Compared with normal chorioretinal tissue (Figures 3A–3C), mTOR expression was upregulated throughout the entire neural retina and the subretinal CNV lesion induced via laser photocoagulation (Figures 3D–3F). While this mTOR expression pattern did not change upon the intravitreal administration of rAAV-scrambled shRNA (Figures 3G–3I), it was, however, substantially reduced in the chorioretinal tissue of mice treated with rAAV-mTOR shRNA (Figures 3J–3L).

qRT-PCR analyses showed that mTOR mRNA levels were substantially higher in retinas wherein CNV occurred, as compared with the control (Figures 3M and 3N), with significant reduction observed 14 days after rAAV-mTOR shRNA administration ($p < 0.05$; $n = 5$ for each group).

Anti-angiogenic Effect of rAAV-mTOR shRNA

The anti-angiogenic effect of the rAAV-mTOR shRNA was evaluated by immunostaining the areas where CNV occurred with phalloidin and anti-CD31. We found that animals treated with rAAV-mTOR shRNA exhibited markedly reduced areas of CNV activity when compared with the control group and mice treated with rAAV-scrambled shRNA ($p = 0.028$ and $p = 0.026$, respectively; $n = 5$ for each group) (Figure 4). To more precisely analyze the therapeutic effects of rAAV-mTOR shRNA treatment, we evaluated transverse-sectioned chorioretinal samples of the laser-induced CNV lesions for CD31-positive staining, which showed that, compared with the two other experimental groups, CD31-positive signals were markedly reduced in mice treated with rAAV-mTOR shRNA (Figure 5).

Anti-inflammatory Effect of rAAV-mTOR shRNA

Inflammatory cells, such as macrophages, monocytes, and microglia, play major roles in the development of AMD, particularly when CNV is implicated. As such, we evaluated whether mTOR inhibition via rAAV-mTOR shRNA modulates the proliferation and/or infiltration of inflammatory cells in the development and maturation of laser-induced CNV using anti-CD11b and -F4/80 antibodies on transverse sections of the retina 14 days after laser treatment. Abundant CD11b- and F4/80-positive cells were observed around CNV lesions in the subretinal and intraretinal regions of the mice injected with 0.1% PBS and rAAV-scrambled shRNA (Figures 6A–6F and 6J–6O). However, significantly less inflammatory cell infiltration was observed in retinas treated with rAAV-mTOR shRNA when compared with the control group and with mice treated with rAAV-scrambled shRNA (CD11b: $p = 0.036$ and $p = 0.016$, respectively; F4/80: $p = 0.027$ and $p = 0.022$, respectively; $n = 5$ for each group; Figures 6G–6I and 6P–6R). Specifically, the number of F4/80-positive cells was 42.4 ± 10.4 in rAAV-mTOR shRNA-treated retinas, 82.8 ± 10.0 in rAAV-scrambled shRNA-treated retinas, and 84.4 ± 17.0 in the untreated group; the number of CD11b-positive cells was 90.0 ± 11.6, 127.6 ± 14.4, and 123.8 ± 13.0, respectively (Figures 6S and 6T).

Autophagy in Laser-Induced CNV

To evaluate whether the induction of autophagy via mTOR inhibition is involved in CNV regression, we immunostained chorioretinal tissues for the autophagy markers LC3B and ATG7. Activation of autophagy was detected via both LC3B and ATG7 immunostaining 14 days after laser photocoagulation in the CNV lesions of retinas treated with rAAV-mTOR shRNA. In 0.1% PBS and rAAV-scrambled shRNA-treated mice, only background LC3B and weakly positive ATG7 signals were observed (Figure 7).

Cell Apoptosis around Laser-Induced CNV

At 14 days after laser photocoagulation, the terminal deoxynucleotidyl transferase-mediated biotinylated deoxyuridine triphosphate (dUTP) nick end labeling (TUNEL) assay was used to determine the number of apoptotic cells observed in the outer nuclear layer (ONL) and around the CNV of all three experimental groups. Significantly fewer TUNEL-positive cells were found in the ONL of rAAV-mTOR shRNA-treated retinas when compared with mice injected with 0.1% PBS and rAAV-scrambled shRNA ($p = 0.038$ and $p = 0.024$, respectively; $n = 5$ for each group). Specifically, the number of TUNEL-positive cells was 8.4 ± 3.0 for rAAV-mTOR shRNA-treated retinas, 19.4 ± 4.0 for rAAV-scrambled shRNA-treated retinas, and 17.8 ± 4.8 in untreated control retinas (Figure 8).

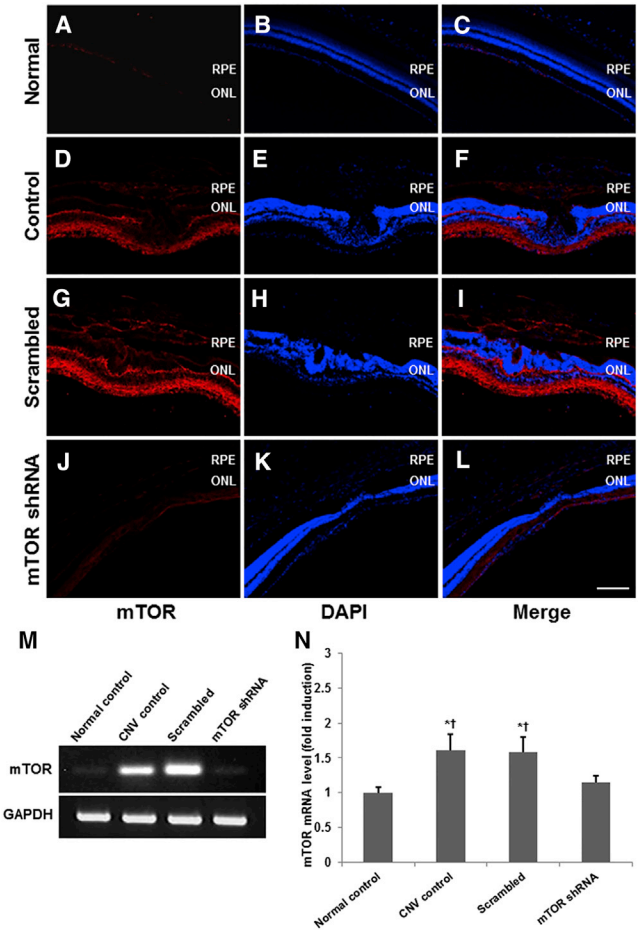

Figure 3. mTOR Expression Resulting from Laser-Induced CNV

(A–L) Compared with normal chorioretinal tissue, mTOR expression was upregulated throughout the neural retina and subretinal CNV lesions for both 0.1% PBS-injected control eyes (A–F) and rAAV-scrambled shRNA-injected eyes (G–I), whereas mice treated with mTOR shRNA showed substantially reduced mTOR expression throughout (J–L). (M and N) Quantitative analyses were conducted using RT-PCR. mTOR mRNA levels were substantially increased upon the formation of CNV and subsequently reduced significantly upon the intravitreal administration of rAAV-mTOR shRNA. Data are presented as mean ± SEM. Asterisk indicates statistically significant (*$p < 0.05$) differences versus the control. Cross indicates statistically significant (†$p < 0.05$) differences versus the rAAV-mTOR shRNA-treated group. Scale bar, 100 μm. ONL, outer nuclear layer; RPE, retinal pigment epithelium.

DISCUSSION

Building upon previous research targeting the mTOR signaling pathway as a therapeutic for various diseases, a number of studies have investigated the role of mTOR in the pathological conditions of the retina.[15–17,19,29,30] Using mTOR pathway inhibitors, recently it has been shown that blocking mTOR signaling conferred protection against the formation and progression of CNV.[16,18,19,30] Most of these studies, however, utilized rapamycin and/or temsirolimus, a rapamycin analog, both of which inhibit mTORC1 while activating mTORC2 via a negative feedback loop. These opposing effects hinder the comprehensive investigation of the therapeutic potential of mTOR inhibition. In comparison, we were here able to block both mTORC1 and mTORC2 simultaneously by utilizing siRNA to selectively target mTOR itself. To the best of our knowledge, the use of these siRNAs, incorporated into rAAV as an shRNA, represents the first study to simultaneously affect both mTORC complexes to demonstrate the therapeutic effects of mTOR inhibition on CNV development. We found that intravitreally administered rAAV-mTOR shRNA successfully transduced various cells in CNV lesions and suppressed the progression of CNV. Significantly elevated autophagy levels were detectable in rAAV-mTOR shRNA-treated mouse retinas when compared with animals injected with an rAAV-scrambled shRNA or 0.1% PBS as a control. Furthermore, the retinas of rAAV-mTOR shRNA-treated mice exhibited markedly reduced apoptosis activity.

Among the well-established roles of mTOR are the regulation of cellular metabolism and cell growth during development or after injury. Neuronal mTOR activity decreases over the course of development in the murine CNS, and only limited activity is observable in the adult CNS.[31,32] mTOR expression is restricted to the ganglion cell layer and inner nuclear layer (INL) of normal mouse retinas,[33,34] and our results correspond with these earlier findings. Furthermore, we confirm here that mTOR expression is significantly increased in the CNV-induced retinas, particularly the inner plexiform retinal layer and the CNV lesion itself. Because mTOR immunoreactivity was shown to be downregulated in normal mouse retinas, we speculate that shRNA-mediated mTOR inhibition does not affect the viability of normal retinal cells, and that it has inhibitory effects only upon cells with upregulated mTOR expression.

One of the major novel findings in this study is that intravitreally administered rAAV-mTOR shRNA successfully transduced cells in CNV lesions in mouse retinas induced via laser photocoagulation. Although numerous studies have shown that the AAV-mediated delivery of therapeutic genes may inhibit CNV formation,[35–37] none has demonstrated the direct transduction of AAV into cells of CNV lesions. Here, we report that rAAV-mTOR shRNA effectively transduces endothelial cells, the main cellular components of CNV. Combined with other results, we posit that the inhibition of the mTOR pathway in endothelial and inflammatory cells may play a crucial role in limiting CNV formation, with long-lasting therapeutic effects achievable via a single intravitreal administration of rAAV-mTOR shRNA capable of directly transducing cells in the CNV lesions themselves.

Several pathophysiological factors have previously been linked with AMD, primarily inflammation and angiogenesis.[38,39] A number of previous studies have documented that both mTORC1 and mTORC2 are involved in angiogenesis and pro-inflammatory processes, and that the inhibition of the mTOR pathway may have anti-inflammatory and anti-angiogenic effects.[12,14,30,40–43] The rAAV-mTOR shRNA used in this study inhibits both mTOR complexes, leading to the profound suppression of inflammation and angiogenesis, confirmed by immunohistology utilizing CD11b, F4/80, and CD31. These revealed that rAAV-mTOR shRNA-treated mouse retinas

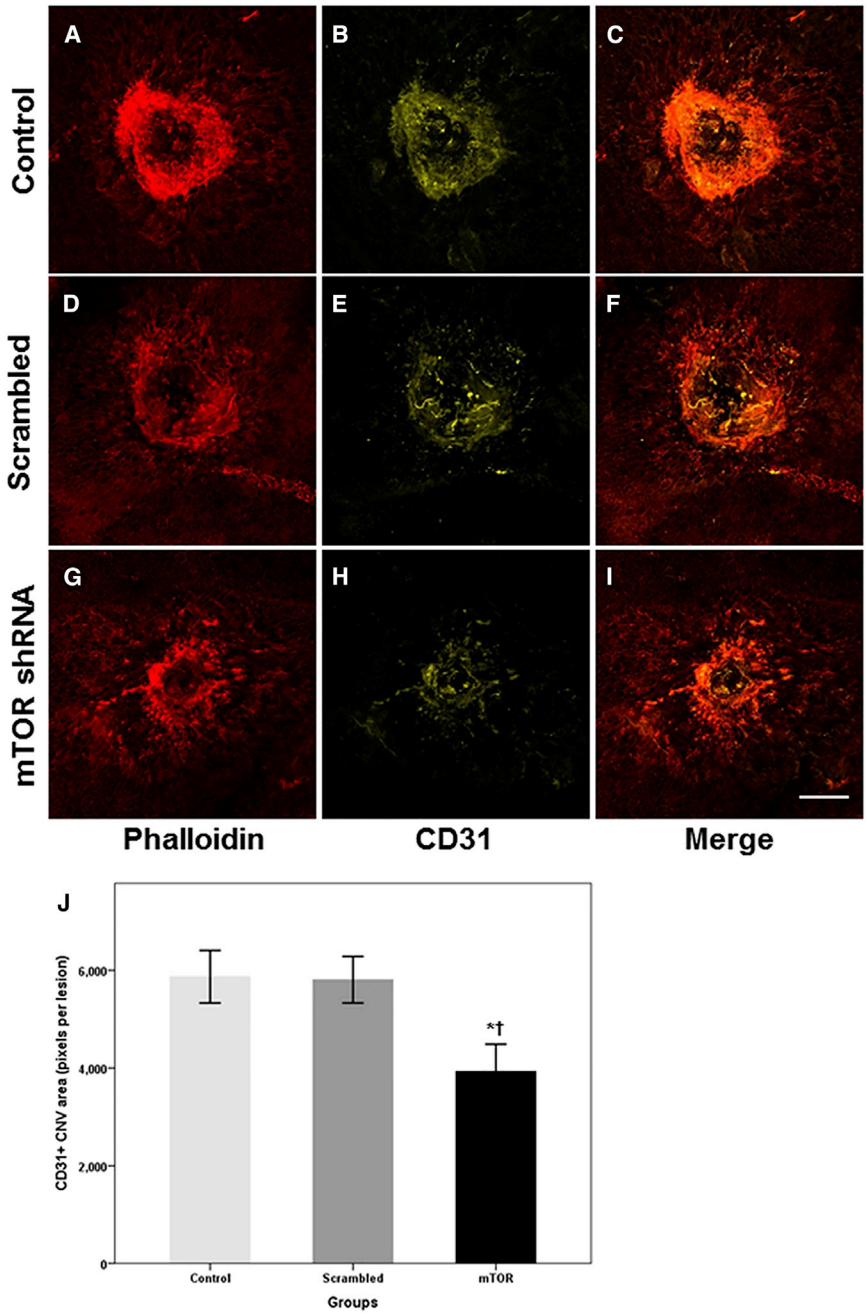

Figure 4. Immunohistochemistry of Phalloidin and CD31 for Endothelial Cells Resulting from Laser-Induced CNV

The extensiveness of the CNV was measured via whole-mount phalloidin (red) and CD31 (yellow) immunostains. (A–I) Whereas the areas where CNV occurred were widespread for the control and scrambled shRNA-treated groups (A–F), CNV was substantially reduced for mice treated with mTOR shRNA (G–I). Bar graph shows CNV extent, as measured by pixels per lesion, using the Kruskal-Wallis test with post hoc analysis (J, mean ± SEM). Asterisk indicates statistically significant differences versus the control (*$p < 0.05$). Cross (†) indicates statistically significant differences versus the scrambled shRNA-treated group. Scale bars, 100 μm.

exhibited a reduction in the extent of CNV lesions and significantly less infiltration by monocytes and macrophages. Additionally, as the secretion of various cytokines and chemokines, such as IL-1β and TNF-α,[44] further activates endothelial cells in the early stages of inflammation, the anti-inflammatory effects of mTOR inhibition may also be implicated in reducing angiogenesis.

To date, there is strong evidence to support that impaired autophagy in the RPE leads to the accumulation of lipofuscin and a reduced ability to clear intracellular debris,[45–48] and that the activation of autophagy, modulated by the rapamycin-induced inhibition of mTORC1, is able to prevent this harmful AMD-related aging of RPE cells.[18–20] As seen in the expression of LC3B and ATG7, selective markers for autophagic activity, we demonstrate here that this specific mode of autophagy activation significantly reduces CNV. LC3B expression was detected mainly in the CNV lesions themselves, and with the clearly observable transduction of rAAV-mTOR shRNA into the lesions, it is highly likely that this site-specific activation of autophagy was due to the inhibitory effects of mTOR shRNA on mTOR signaling. Moreover, by increasing autophagy in the CNV lesions, mTOR inhibition may not only limit CNV progression, but also reverse previous CNV activity. Therefore, treatments resulting in enhanced autophagy via mTOR inhibition may help overcome the limitations of the anti-VEGF therapies currently used, which work by decreasing vascular permeability and inhibiting new vessel formation, but have a limited effect on stable mature vessels covered with pericytes.[49–51]

In addition to CNV formation, AMD is characterized by RPE degeneration and the loss of photoreceptors. It was previously reported that mTOR inhibition by rapamycin prevents pathological changes in RPE cells and protects photoreceptors from oxidative stress.[52] Correspondingly, the TUNEL assay showed that rAAV-mTOR shRNA treatment, which unlike the variable activity of rapamycin with respect to the two mTOR complexes, affects both mTORC1 and mTORC2, and significantly reduced apoptosis activity in ONL cells around the CNV when compared with controls. Although beyond the scope of the current manuscript, if mTOR inhibition is directly responsible for protecting photoreceptors and is not due to the effects

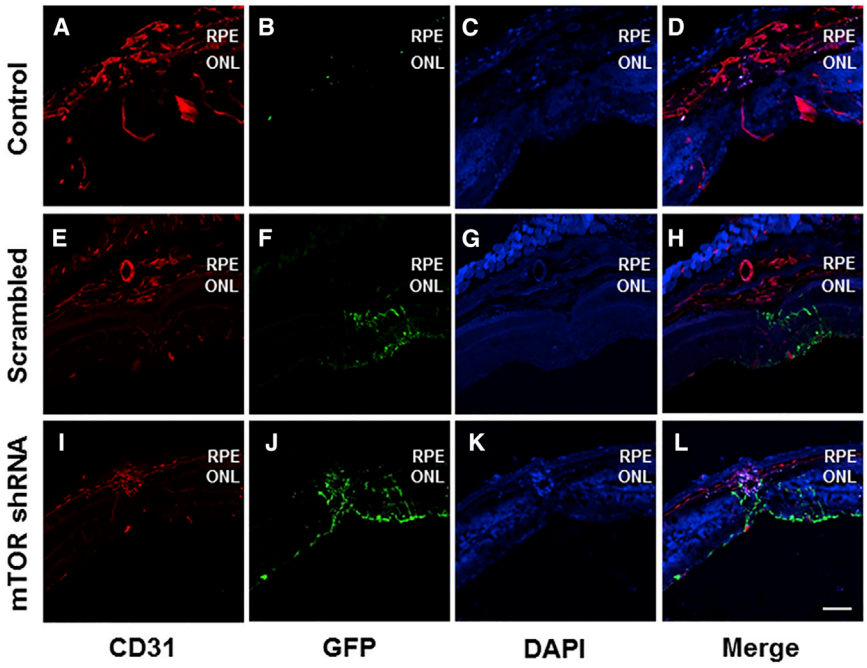

Figure 5. Transverse Retinal Sections Immunolabeled with CD31 and GFP

(A–L) CD31 (red) expression was detectable throughout the laser-induced CNV lesions in the retinas of the control- (A–D) and rAAV-scrambled shRNA-treated groups (E–H), while CD31 expression was markedly reduced in the rAAV-mTOR shRNA-treated group (I–L). (F and J) Substantial GFP (green) expression exhibited in the rAAV-scrambled shRNA- and rAAV-mTOR shRNA-treated groups (F and J) indicated the effective transducing qualities of the viral vector. Scale bar, 100 μm. ONL, outer nuclear layer; RPE, retinal pigment epithelium.

to rapamycin, this additional aspect of rAAV-mTOR shRNA treatment may increase its efficacy as an AMD therapeutic.

In summation, we demonstrate here that mTOR inhibition mediated by rAAV-mTOR shRNA in a mouse model for AMD resulted in increased autophagic activity, reduced inflammatory activity, and reduced angiogenesis in laser-induced CNV lesions, as well as an overall reduction in the extent of CNV. In addition to being able to effectively transduce CNV lesions because of its scAAV2 packaging vector, the mTOR-targeting shRNA was designed to be multispecies compatible. Therefore, rAAV-mTOR shRNA may serve as the foundation for the development of therapeutics to replace or to be used in conjunction with the anti-VEGF therapies currently used to treat AMD. Further preclinical studies will be necessary to determine the optimal concentration of the therapeutic vector to maximize efficacy and to evaluate ocular and systemic toxicity with regard to dose escalation.

MATERIALS AND METHODS

Animals

Eight-week-old male C57/BL6 mice (The Orient Bio) were used in this study. All animal care and experiments were performed in accordance with the guidelines in the Association for Research in Vision and Ophthalmology Resolution on the Use of Animals in Ophthalmic and Vision Research and overseen by the Institutional Animal Care and Use Committee of Soonchunhyang University Hospital Bucheon.

Laser-Induced CNV

After anesthetizing the animals via the intraperitoneal (i.p.) injection of a mixture of 40 mg/kg zolazepam/tiletamine (Zoletil; Virbac) and 5 mg/kg xylazine (Rompun; Bayer Healthcare), the pupils were dilated with 0.5% tropicamide and 2.5% phenylephrine (Mydrin-P; Santen). Laser photocoagulation (200 μm spot size, 0.02 s duration, 100 mW) was performed using a PASCAL diode ophthalmic laser system (neodymium-doped yttrium aluminium garnet [Nd:YAG], 532 nm; Topcon Medical Laser Systems). Only the right eye of each mouse was exposed to laser photocoagulation to induce CNV. Five to six laser spots were applied around the optic nerve head of said eye. A gaseous bubble formed at each laser spot, indicating the rupture of Bruch's membrane.

Preparation of rAAV-mTOR shRNA-EGFP and Intravitreal Injections

All recombinant AAV vectors were derived from scAAV2 vectors. The mTOR siRNA (5′-GAAUGUUGACCAAUGCUAU-3′) was designed from the completely conserved multi-species region found in humans (NM_004958), monkeys (XR_014791), rats (NM_019906), and mice (NM_020009) to establish rAAV-mTOR shRNA-EGFP. A scrambled control siRNA (5′-AUUCUAUCACUAGCGUGAC-3′) was prepared to make rAAV-scrambled control shRNA-EGFP (rAAV-scrambled shRNA-EGFP). Both of the scAAV2 vectors use the H1 promoter to express either mTOR siRNA or the scrambled control siRNA, whereas EGFP expression is driven by the cytomegalovirus promoter. All rAAV vectors were supplied by CdmoGen. Intravitreal injections of the vector were performed in the right eyes of the mice, with pupil dilation, 5 days after laser photocoagulation under anesthesia using 35G blunt needles with Nanofil syringes (World Precision Instruments). One microliter of the viral vectors at a concentration of 5.0×10^{10} viral genomes (vg)/mL was used per injection. Laser photocoagulation was used to induce CNV in three groups of mice (n = 20 per each group) before being injected with the following: 0.1% PBS for the first group, rAAV-scrambled shRNA for the second, and rAAV-mTOR shRNA for the third. As a negative control, 10 mice were not treated with laser photocoagulation or intravitreal injections. Five mice from each group were used for qRT-PCR.

FFA

FFA was performed using a scanning laser ophthalmoscope (Heidelberg Retina Angiograph 2; Heidelberg Engineering) as previously

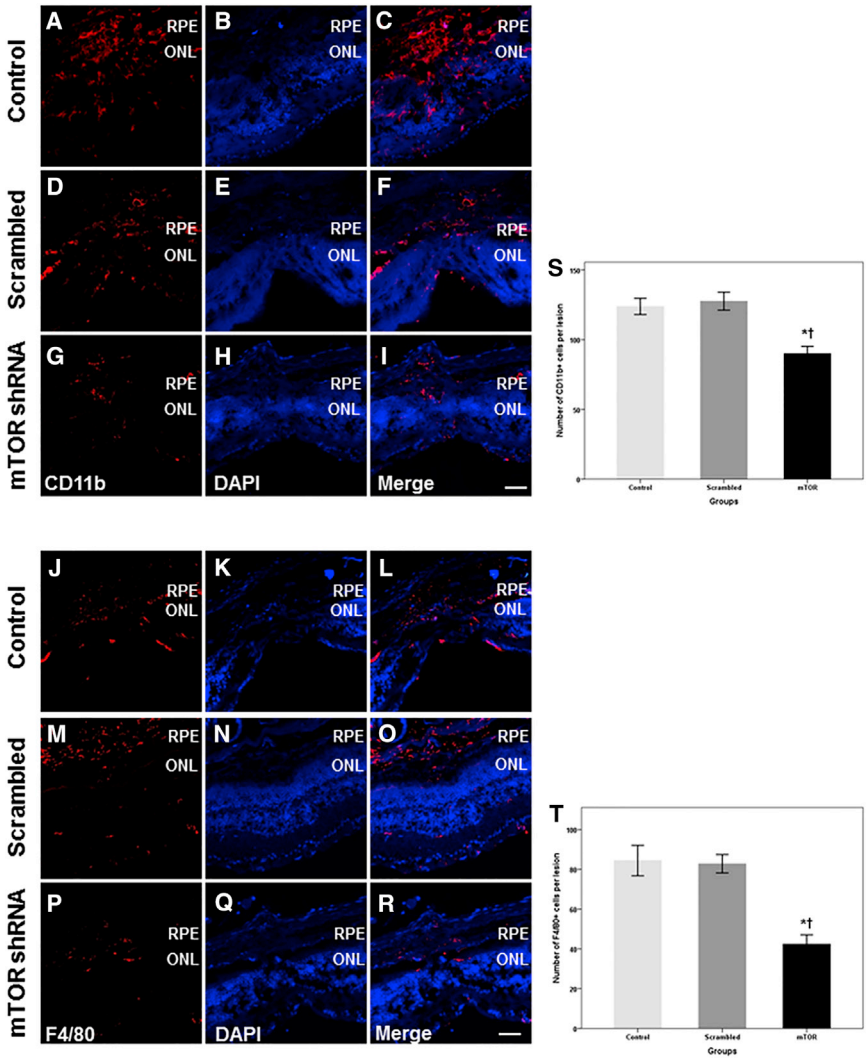

Figure 6. Representative Confocal Images of CD11b and F4/80 Immunostaining and Quantitative Analyses of Inflammatory Cell Infiltration

(A–F and J–O) Immunohistochemistry with CD11b and F4/80 revealed the extensive presence of inflammatory cells in the retinas of mice injected with 0.1% PBS and rAAV-scrambled shRNA. (G–I and P–R) In contrast, significantly fewer CD11b- and F4/80-positive inflammatory cells were found in the animals treated with rAAV-mTOR shRNA. (S and T) Significantly fewer CD11b- (S) and F4/80-positive cells (T) were seen in the rAAV-mTOR shRNA-treated group when compared with the control and rAAV-scrambled shRNA-treated groups (CD11b: $p = 0.036$ and $p = 0.016$, respectively; F4/80: $p = 0.027$ and $p = 0.022$, respectively). Data are presented as mean ± SEM. Asterisk indicates statistically significant differences versus the control (*$p < 0.05$). Cross (†) indicates statistically significant differences versus the rAAV-scrambled shRNA-treated group. Scale bars, 100 μm. ONL, outer nuclear layer; RPE, retinal pigment epithelium.

described.[53] In brief, the animal was anesthetized and the pupil dilated to observe the retina. FFA images were captured 3–5 min after an i.p. injection with 0.1 mL of 2% fluorescein sodium (Fluorescite; Akorn). FFA was performed at 5 and 13 days post-laser photocoagulation.

Tissue Preparation

The mice were deeply anesthetized via an intraperitoneal injection of a 4:1 mixture of zolazepam/tiletamine (80 mg/kg) and xylazine (10 mg/kg), then intracardially perfused with 0.1 M PBS containing 150 U/mL heparin, followed by an infusion of 4% paraformaldehyde (PFA) in 0.1 M phosphate buffer (PB). After ocular enucleation, the anterior segment, including the cornea and lens, was removed to generate eyecups. For RPE whole mounts, the neural retina was removed as well. The RPE-choroid complex was fixed with 4% PFA in 0.1 M PB (pH 7.4) for 2 hr and prepared with four equidistant cuts. To prepare frozen sectioned samples, we fixed eyecups with attached neural retinas with 4% PFA in 0.1 M PB (pH 7.4) for 2 hr. The eyecups were then transferred to 30% sucrose in PBS, incubated overnight, and embedded in optimal cutting temperature (OCT) compound (Sakura Finetek). Using the embedded eyecups, serial sagittal sections 10 μm thick were prepared and the sections mounted on adhesive microscope slides (HistoBond; Marienfeld-Superior). Transverse sections with CNV lesions were selected among the samples by visually scanning all serial sections.

Immunohistochemistry

Immunohistochemistry was performed for both whole mounts and transverse sections of the retina. To immunostain whole mounts, we incubated RPE-choroid tissues overnight at 4°C with anti-CD31 (550274, 1:200; BD Pharmingen) diluted in PBS containing 1% Triton X-100 (PBST; Sigma-Aldrich). The tissues were washed three times for 10 min apiece with PBST and incubated for 2 hr at room temperature with Alexa Fluor 532-conjugated goat anti-mouse (A11002; Thermo Fisher Scientific) and rhodamine-conjugated phalloidin (A22287; Thermo Fisher Scientific). For transverse sections, slides were incubated overnight at 4°C with primary antibodies for either anti-CD11b (MCA711G, 1:200; Serotec), anti-F4/80 (MCA497GA, 1:200; Serotec), or anti-CD31 (550274, 1:200; BD Pharmingen) to detect monocyte, macrophage, and endothelial cells, respectively. To visualize EGFP expression and verify transduction by the AAVs, we used an anti-GFP antibody (ab6556, 1:200; Abcam). mTOR or autophagy activity was observed using anti-mTOR (AF15371, 1:200; R&D Systems) and anti-LC3B IgG (NB110-2220, 1:200; Novus Biologicals), respectively. For the TUNEL assay, the tissue was stained in accordance with the protocol provided by the manufacturer (12156792910, In Situ Cell Death Detection Kit, TMR red; Roche Diagnostics). After washing three times with PBST, the samples

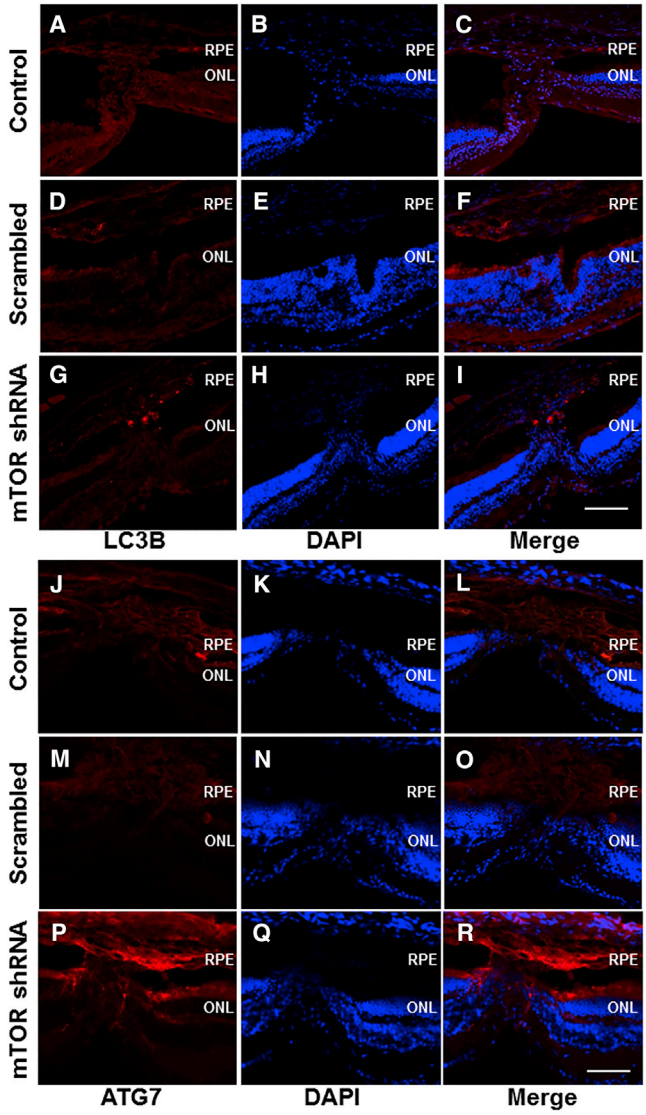

Figure 7. Immunolabeling for Autophagy Using Autophagy Markers LC3B and ATG7

(G–I and P–R) Immunostaining against LC3B and ATG7 was used to detect autophagy, which was mainly found in the rAAV-mTOR shRNA-treated group. (A–F and J–O) On the other hand, only background LC3B and weak, lesion-confined ATG7 expression were detected in the control (A–C and J–L) and rAAV-mTOR scrambled-treated groups (D–F and M–O). Scale bars, 100 μm. ONL, outer nuclear layer; RPE, retinal pigment epithelium.

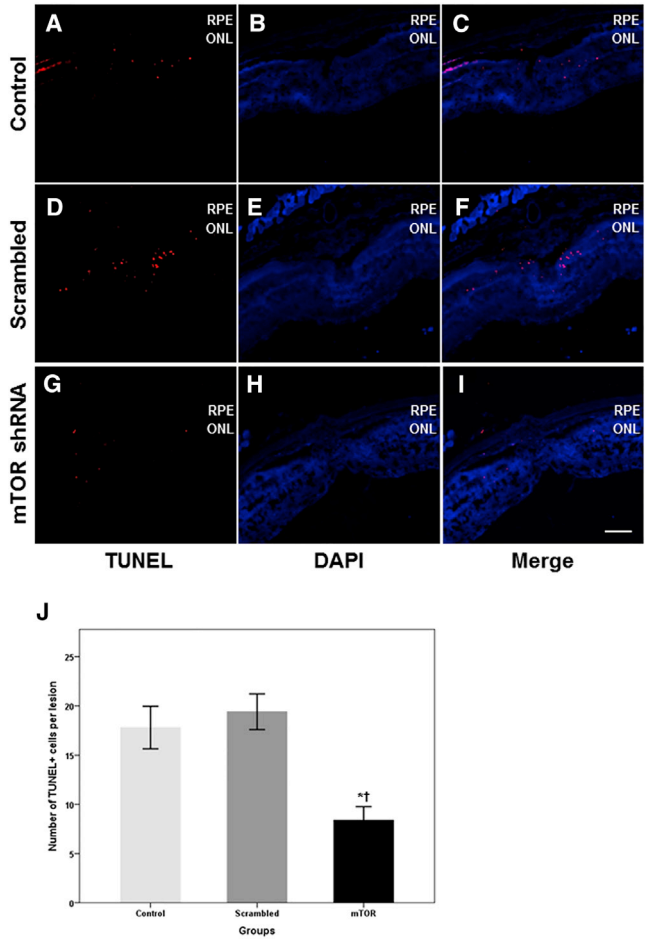

Figure 8. Analyses of Apoptotic Cells via TUNEL Assay

(A–I) TUNEL-positive cells were found in the outer nuclear layer (ONL) and around the CNV lesions of the control (A–C), rAAV-scrambled shRNA-treated (D–F), and rAAV-mTOR shRNA-treated groups (G–I), with the latter containing noticeably fewer apoptotic cells. (J) As seen in the summarized data, significantly fewer TUNEL-positive cells were detected in the ONL of rAAV-mTOR shRNA-treated retinas when compared with the control and rAAV-scrambled shRNA-treated groups ($p = 0.038$ and $p = 0.024$, respectively). Data are presented as mean ± SEM. Asterisk indicates statistically significant differences versus the control (*$p < 0.05$). Cross (†) indicates statistically significant differences versus the rAAV-scrambled shRNA-treated group. Scale bars, 100 μm. ONL, outer nuclear layer; RPE, retinal pigment epithelium.

were incubated with Alexa Fluor 488-, 546-, and 647-conjugated (Thermo Fisher Scientific) secondary antibodies and stained with DAPI (D9542; Sigma-Aldrich) to visualize the cell nuclei. Both the whole mounts and transverse sections were examined via fluorescence confocal microscopy (LSM 700; Carl Zeiss Microscopy), with images captured using image-capture software (LSM Image Browser; Carl Zeiss Microscopy) at ×100 and ×200 magnification.

RT-PCR

The eyeball was enucleated from deeply anesthetized mice, and the cornea, lens, and RPE-choroid complex were removed. Total RNA was prepared from the neural retina without the RPE-choroid complex using TRIzol reagent (Invitrogen). RNA (2 μg) was reverse transcribed into cDNA using Superscript III (Invitrogen). Samples were analyzed for mRNA levels using SYBR Green kits (Invitrogen), and fold changes in mRNA expression were determined using the $2^{-\Delta\Delta Ct}$ method, normalizing the results to the expression of the control *GAPDH*. PCR was carried out in triplicate, with amplification

performed utilizing a pair of primers specific for mTOR (forward: 5′-CCACTGTGCCAGAATCCATC-3′, reverse: 5′-GAGAAATCCC GACCAGTGAG-3′).

Image Analysis and Statistical Analysis

Data collection for quantitative comparisons of the extent of CNV and cell counts for monocyte, macrophage, and TUNEL-positive cells was conducted using ImageJ software (NIH). For counting cells, five transverse sections from each CNV lesion were selected and immunostaining-positive cells counted at ×100 magnification. Five laser-induced CNV lesions from each group were included for each analysis, with statistical analyses performed using SPSS software (version 20.0 for Windows; SPSS). The Kruskal-Wallis test with a post hoc analysis (Bonferroni's method) was used for the comparison, and significant difference was determined at $p < 0.05$.

AUTHOR CONTRIBUTIONS

Conceptualization, T.K.P. and K.P.; Methodology, T.K.P. and J.S.C.; Investigation, T.K.P., S.H.L., J.S.C., S.K.N., H.J.K., and H.Y.P.; Writing – Original Draft, T.K.P. and S.H.L.; Writing – Review & Editing, T.K.P., K.P. S.H.L., S.H.S.L., and J.S.C.; Supervision, T.K.P., H.L. and K.P.

CONFLICTS OF INTEREST

No potential conflicts of interest exist for all authors.

ACKNOWLEDGMENTS

This work was supported in part by the Soonchunhyang University Research Fund.

REFERENCES

1. Klein, R., Klein, B.E., Jensen, S.C., and Meuer, S.M. (1997). The five-year incidence and progression of age-related maculopathy: the Beaver Dam Eye Study. Ophthalmology *104*, 7–21.
2. Haddad, S., Chen, C.A., Santangelo, S.L., and Seddon, J.M. (2006). The genetics of age-related macular degeneration: a review of progress to date. Surv. Ophthalmol. *51*, 316–363.
3. Zarbin, M.A. (2004). Current concepts in the pathogenesis of age-related macular degeneration. Arch. Ophthalmol. *122*, 598–614.
4. Kaiser, P.K. (2013). Emerging therapies for neovascular age-related macular degeneration: drugs in the pipeline. Ophthalmology *120* (5 Suppl), S11–S15.
5. van Wijngaarden, P., and Qureshi, S.H. (2008). Inhibitors of vascular endothelial growth factor (VEGF) in the management of neovascular age-related macular degeneration: a review of current practice. Clin. Exp. Optom. *91*, 427–437.
6. Day, S., Acquah, K., Lee, P.P., Mruthyunjaya, P., and Sloan, F.A. (2011). Medicare costs for neovascular age-related macular degeneration, 1994-2007. Am. J. Ophthalmol. *152*, 1014–1020.
7. Laplante, M., and Sabatini, D.M. (2012). mTOR signaling in growth control and disease. Cell *149*, 274–293.
8. Markman, B., Dienstmann, R., and Tabernero, J. (2010). Targeting the PI3K/Akt/mTOR pathway–beyond rapalogs. Oncotarget *1*, 530–543.
9. Perluigi, M., Di Domenico, F., and Butterfield, D.A. (2015). mTOR signaling in aging and neurodegeneration: at the crossroad between metabolism dysfunction and impairment of autophagy. Neurobiol. Dis. *84*, 39–49.
10. Willems, L., Tamburini, J., Chapuis, N., Lacombe, C., Mayeux, P., and Bouscary, D. (2012). PI3K and mTOR signaling pathways in cancer: new data on targeted therapies. Curr. Oncol. Rep. *14*, 129–138.
11. Kim, Y.C., and Guan, K.L. (2015). mTOR: a pharmacologic target for autophagy regulation. J. Clin. Invest. *125*, 25–32.
12. Aimi, F., Georgiopoulou, S., Kalus, I., Lehner, F., Hegglin, A., Limani, P., Gomes de Lima, V., Rüegg, M.A., Hall, M.N., Lindenblatt, N., et al. (2015). Endothelial Rictor is crucial for midgestational development and sustained and extensive FGF2-induced neovascularization in the adult. Sci. Rep. *5*, 17705.
13. Saxton, R.A., and Sabatini, D.M. (2017). mTOR signaling in growth, metabolism, and disease. Cell *168*, 960–976.
14. Farhan, M.A., Carmine-Simmen, K., Lewis, J.D., Moore, R.B., and Murray, A.G. (2015). Endothelial cell mTOR complex-2 regulates sprouting angiogenesis. PLoS ONE *10*, e0135245.
15. Yagasaki, R., Nakahara, T., Ushikubo, H., Mori, A., Sakamoto, K., and Ishii, K. (2014). Anti-angiogenic effects of mammalian target of rapamycin inhibitors in a mouse model of oxygen-induced retinopathy. Biol. Pharm. Bull. *37*, 1838–1842.
16. Liegl, R., Koenig, S., Siedlecki, J., Haritoglou, C., Kampik, A., and Kernt, M. (2014). Temsirolimus inhibits proliferation and migration in retinal pigment epithelial and endothelial cells via mTOR inhibition and decreases VEGF and PDGF expression. PLoS ONE *9*, e88203.
17. Lin, C.H., Li, C.H., Liao, P.L., Tse, L.S., Huang, W.K., Cheng, H.W., and Cheng, Y.W. (2013). Silibinin inhibits VEGF secretion and age-related macular degeneration in a hypoxia-dependent manner through the PI-3 kinase/Akt/mTOR pathway. Br. J. Pharmacol. *168*, 920–931.
18. Zhang, J., Bai, Y., Huang, L., Qi, Y., Zhang, Q., Li, S., Wu, Y., and Li, X. (2015). Protective effect of autophagy on human retinal pigment epithelial cells against lipofuscin fluorophore A2E: implications for age-related macular degeneration. Cell Death Dis. *6*, e1972.
19. Mitter, S.K., Song, C., Qi, X., Mao, H., Rao, H., Akin, D., Lewin, A., Grant, M., Dunn, W., Jr., Ding, J., et al. (2014). Dysregulated autophagy in the RPE is associated with increased susceptibility to oxidative stress and AMD. Autophagy *10*, 1989–2005.
20. Yao, J., Jia, L., Khan, N., Lin, C., Mitter, S.K., Boulton, M.E., Dunaief, J.L., Klionsky, D.J., Guan, J.L., Thompson, D.A., and Zacks, D.N. (2015). Deletion of autophagy inducer RB1CC1 results in degeneration of the retinal pigment epithelium. Autophagy *11*, 939–953.
21. Feuer, W.J., Schiffman, J.C., Davis, J.L., Porciatti, V., Gonzalez, P., Koilkonda, R.D., Yuan, H., Lalwani, A., Lam, B.L., and Guy, J. (2016). Gene therapy for Leber hereditary optic neuropathy: initial results. Ophthalmology *123*, 558–570.
22. Bainbridge, J.W., Smith, A.J., Barker, S.S., Robbie, S., Henderson, R., Balaggan, K., Viswanathan, A., Holder, G.E., Stockman, A., Tyler, N., et al. (2008). Effect of gene therapy on visual function in Leber's congenital amaurosis. N. Engl. J. Med. *358*, 2231–2239.
23. Hauswirth, W.W., Aleman, T.S., Kaushal, S., Cideciyan, A.V., Schwartz, S.B., Wang, L., Conlon, T.J., Boye, S.L., Flotte, T.R., Byrne, B.J., and Jacobson, S.G. (2008). Treatment of leber congenital amaurosis due to RPE65 mutations by ocular subretinal injection of adeno-associated virus gene vector: short-term results of a phase I trial. Hum. Gene Ther. *19*, 979–990.
24. Maguire, A.M., Simonelli, F., Pierce, E.A., Pugh, E.N., Jr., Mingozzi, F., Bennicelli, J., Banfi, S., Marshall, K.A., Testa, F., Surace, E.M., et al. (2008). Safety and efficacy of gene transfer for Leber's congenital amaurosis. N. Engl. J. Med. *358*, 2240–2248.
25. Lee, S.H., Colosi, P., Lee, H., Ohn, Y.H., Kim, S.W., Kwak, H.W., and Park, T.K. (2014). Laser photocoagulation enhances adeno-associated viral vector transduction of mouse retina. Hum. Gene Ther. Methods *25*, 83–91.
26. Lee, S.H., Kong, Y.J., Lyu, J., Lee, H., Park, K., and Park, T.K. (2015). Laser photocoagulation induces transduction of retinal pigment epithelial cells by intravitreally administered adeno-associated viral vectors. Hum. Gene Ther. Methods *26*, 159–161.
27. Lee, H.S., Ahn, J., Jun, E.J., Yang, S., Joo, C.H., Kim, Y.K., and Lee, H. (2009). A novel program to design siRNAs simultaneously effective to highly variable virus genomes. Biochem Biophys Res Commun. *384*, 431–435.
28. Ahn, J., Woo, H.N., Ko, A., Khim, M., Kim, C., Park, N.H., Song, H.Y., Kim, S.W., and Lee, H. (2012). Multispecies-compatible antitumor effects of a cross-species small-interfering RNA against mammalian target of rapamycin. Cell. Mol. Life Sci. *69*, 3147–3158.

29. Ma, J., Sun, Y., López, F.J., Adamson, P., Kurali, E., and Lashkari, K. (2016). Blockage of PI3K/mTOR pathways inhibits laser-induced choroidal neovascularization and improves outcomes relative to VEGF-A suppression alone. Invest. Ophthalmol. Vis. Sci. *57*, 3138–3144.

30. Dejneka, N.S., Kuroki, A.M., Fosnot, J., Tang, W., Tolentino, M.J., and Bennett, J. (2004). Systemic rapamycin inhibits retinal and choroidal neovascularization in mice. Mol. Vis. *10*, 964–972.

31. Liu, K., Lu, Y., Lee, J.K., Samara, R., Willenberg, R., Sears-Kraxberger, I., Tedeschi, A., Park, K.K., Jin, D., Cai, B., et al. (2010). PTEN deletion enhances the regenerative ability of adult corticospinal neurons. Nat. Neurosci. *13*, 1075–1081.

32. Park, K.K., Liu, K., Hu, Y., Kanter, J.L., and He, Z. (2010). PTEN/mTOR and axon regeneration. Exp. Neurol. *223*, 45–50.

33. Morgan-Warren, P.J., O'Neill, J., de Cogan, F., Spivak, I., Ashush, H., Kalinski, H., Ahmed, Z., Berry, M., Feinstein, E., Scott, R.A., and Logan, A. (2016). siRNA-mediated knockdown of the mTOR inhibitor RTP801 promotes retinal ganglion cell survival and axon elongation by direct and indirect mechanisms. Invest. Ophthalmol. Vis. Sci. *57*, 429–443.

34. Ma, S., Venkatesh, A., Langellotto, F., Le, Y.Z., Hall, M.N., Rüegg, M.A., and Punzo, C. (2015). Loss of mTOR signaling affects cone function, cone structure and expression of cone specific proteins without affecting cone survival. Exp. Eye Res. *135*, 1–13.

35. Cashman, S.M., Ramo, K., and Kumar-Singh, R. (2011). A non membrane-targeted human soluble CD59 attenuates choroidal neovascularization in a model of age related macular degeneration. PLoS ONE *6*, e19078.

36. Askou, A.L., Pournaras, J.A., Pihlmann, M., Svalgaard, J.D., Arsenijevic, Y., Kostic, C., Bek, T., Dagnaes-Hansen, F., Mikkelsen, J.G., Jensen, T.G., and Corydon, T.J. (2012). Reduction of choroidal neovascularization in mice by adeno-associated virus-delivered anti-vascular endothelial growth factor short hairpin RNA. J. Gene Med. *14*, 632–641.

37. Birke, M.T., Lipo, E., Adhi, M., Birke, K., and Kumar-Singh, R. (2014). AAV-mediated expression of human PRELP inhibits complement activation, choroidal neovascularization and deposition of membrane attack complex in mice. Gene Ther. *21*, 507–513.

38. Ambati, J., and Fowler, B.J. (2012). Mechanisms of age-related macular degeneration. Neuron *75*, 26–39.

39. Kauppinen, A., Paterno, J.J., Blasiak, J., Salminen, A., and Kaarniranta, K. (2016). Inflammation and its role in age-related macular degeneration. Cell. Mol. Life Sci. *73*, 1765–1786.

40. Hu, Y., Lou, J., Mao, Y.Y., Lai, T.W., Liu, L.Y., Zhu, C., Zhang, C., Liu, J., Li, Y.Y., Zhang, F., et al. (2016). Activation of MTOR in pulmonary epithelium promotes LPS-induced acute lung injury. Autophagy *12*, 2286–2299.

41. Huang, S.C., Smith, A.M., Everts, B., Colonna, M., Pearce, E.L., Schilling, J.D., and Pearce, E.J. (2016). Metabolic reprogramming mediated by the mTORC2-IRF4 signaling axis is essential for macrophage alternative activation. Immunity *45*, 817–830.

42. Li, Y., Huang, D., Xia, X., Wang, Z., Luo, L., and Wen, R. (2011). CCR3 and choroidal neovascularization. PLoS ONE *6*, e17106.

43. Stahl, A., Paschek, L., Martin, G., Gross, N.J., Feltgen, N., Hansen, L.L., and Agostini, H.T. (2008). Rapamycin reduces VEGF expression in retinal pigment epithelium (RPE) and inhibits RPE-induced sprouting angiogenesis in vitro. FEBS Lett. *582*, 3097–3102.

44. Lentsch, A.B., and Ward, P.A. (2000). Regulation of inflammatory vascular damage. J. Pathol. *190*, 343–348.

45. Mitter, S.K., Rao, H.V., Qi, X., Cai, J., Sugrue, A., Dunn, W.A., Jr., Grant, M.B., and Boulton, M.E. (2012). Autophagy in the retina: a potential role in age-related macular degeneration. Adv. Exp. Med. Biol. *723*, 83–90.

46. Valapala, M., Wilson, C., Hose, S., Bhutto, I.A., Grebe, R., Dong, A., Greenbaum, S., Gu, L., Sengupta, S., Cano, M., et al. (2014). Lysosomal-mediated waste clearance in retinal pigment epithelial cells is regulated by CRYBA1/βA3/A1-crystallin via V-ATPase-MTORC1 signaling. Autophagy *10*, 480–496.

47. Viiri, J., Amadio, M., Marchesi, N., Hyttinen, J.M., Kivinen, N., Sironen, R., Rilla, K., Akhtar, S., Provenzani, A., D'Agostino, V.G., et al. (2013). Autophagy activation clears ELAVL1/HuR-mediated accumulation of SQSTM1/p62 during proteasomal inhibition in human retinal pigment epithelial cells. PLoS ONE *8*, e69563.

48. Rodríguez-Muela, N., Koga, H., García-Ledo, L., de la Villa, P., de la Rosa, E.J., Cuervo, A.M., and Boya, P. (2013). Balance between autophagic pathways preserves retinal homeostasis. Aging Cell *12*, 478–488.

49. Bergers, G., Song, S., Meyer-Morse, N., Bergsland, E., and Hanahan, D. (2003). Benefits of targeting both pericytes and endothelial cells in the tumor vasculature with kinase inhibitors. J. Clin. Invest. *111*, 1287–1295.

50. Gee, M.S., Procopio, W.N., Makonnen, S., Feldman, M.D., Yeilding, N.M., and Lee, W.M. (2003). Tumor vessel development and maturation impose limits on the effectiveness of anti-vascular therapy. Am. J. Pathol. *162*, 183–193.

51. Cursiefen, C., Chen, L., Borges, L.P., Jackson, D., Cao, J., Radziejewski, C., D'Amore, P.A., Dana, M.R., Wiegand, S.J., and Streilein, J.W. (2004). VEGF-A stimulates lymphangiogenesis and hemangiogenesis in inflammatory neovascularization via macrophage recruitment. J. Clin. Invest. *113*, 1040–1050.

52. Zhao, C., Yasumura, D., Li, X., Matthes, M., Lloyd, M., Nielsen, G., Ahern, K., Snyder, M., Bok, D., Dunaief, J.L., et al. (2011). mTOR-mediated dedifferentiation of the retinal pigment epithelium initiates photoreceptor degeneration in mice. J. Clin. Invest. *121*, 369–383.

53. Han, J.W., Lyu, J., Park, Y.J., Jang, S.Y., and Park, T.K. (2015). Wnt/β-catenin signaling mediates regeneration of retinal pigment epithelium after laser photocoagulation in mouse eye. Invest. Ophthalmol. Vis. Sci. *56*, 8314–8324.